Histopathologic and quantitative autoradiographic study: Histological examination by hematoxylin and eosin staining and Van Gieson staining showed loss of myofibers and infiltration of white blood cells in the infarcted area (Figure 1A-1C, upper and lower panels). Autoradiography revealed a high level of ^{111}In-anti-TNC-Fab radioactivity in the granulation tissue around the necrotic area in the acute MI rats 5 days after producing MI (Figure 1C, upper panel), which corresponds to the localization of TNC molecule detected by immunohistochemistry (Figure 2). The regions of high accumulation of ^{111}In-anti-TNC-Fab in autoradiography coincided with the border zone of acute MI (Figure 1C, upper panel). In the sham-operated rats, accumulation of radioactivity was observed in a small part of the epicardial region, which was adjacent to the area of chest operated on (Figure 1A-1C, middle panels). The average of autoradiographic intensity of ^{111}In-anti-TNC-Fab in the infarcted area was 164.7 photostimulated luminescence (PSL)/mm^2, and 41.9 PSL/mm^2 in the noninfarcted area. The ratio of autoradiographic intensities of ^{111}In-anti-TNC-Fab of infarcted area to noninfarcted area was 3.93, indicating a rich accumulation of ^{111}In-anti-TNC-Fab in the infarcted area. On the other hand, the average autoradiographic intensity of ^{111}In-nonspe-

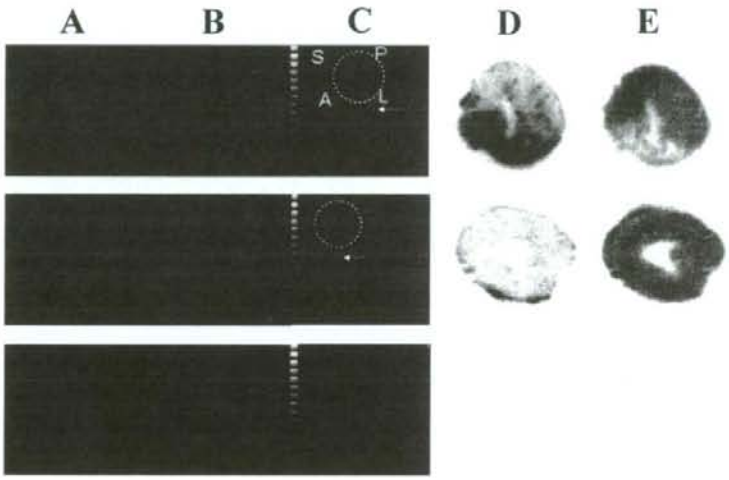

Figure 3. Comparison of SPECT imaging between ^{111}In-anti-TNC-Fab and ^{99m}Tc-MIBI. Transverse dual-isotope SPECT images (**A-C**) and autoradiographies of the same rats (**D**, **E**). The uptake of ^{111}In-anti-TNC-Fab (red in **A**, **C**, **D**) and ^{99m}Tc-MIBI (green in **B**, **C**, **E**) in acute MI heart (upper panels), in sham-operated heart (middle panels), and in normal rat heart (lower panels). **A** indicates anterior left ventricular wall; L, lateral left ventricular wall; P, posterior left ventricular wall; and S, septal wall. Red color indicates the uptake of ^{111}In-anti-TNC-Fab and green color, the uptake of ^{99m}Tc-MIBI. Yellow broken lines circle myocardium. White arrows indicate sutured incision of the left intercostal space just below the myocardium.

Table II. Number of Rats According to Cardiac Repair Diagnosed by ^{111}In-Anti-Tenascin-C-Fab and Myocardial Infarction Diagnosed by ^{99m}Tc-MIBI

		^{99m}Tc-MIBI	
		Myocardial infarction	No infarction
^{111}In-anti-tenascin-C-Fab	Cardiac repair	5	1
	No repair	0	2

cific Fab in the infarcted area was 104.4 PSL/mm^2, while that of the noninfarcted area was 67.3 PSL/mm^2 (Figure 1C, lower panel). The ratio of autoradiographic intensities of ^{111}In-nonspecific Fab of infarcted area to noninfarcted area was 1.55.

In vivo SPECT imaging: Finally, the 5 acute MI rats (3 days after producing MI) and the 3 sham-operated rats were examined to determine whether or not ^{111}In-anti-TNC-Fab could be used to detect *in vivo* myocardial injury. The radiochemical purity of ^{111}In-anti-TNC-Fab was higher than 90%. *In vivo* dual-isotope SPECT imaging showed the complementary uptake of ^{111}In-anti-TNC-Fab (Figure 3A, 3C, red in upper panels) and ^{99m}Tc-MIBI (Figure 3B, 3C, green in upper panels). No specific myocardial uptake of ^{111}In-anti-TNC-Fab was observed in sham-operated rats, although there was some uptake in the operated chest (Figure 3A-3C, middle panels). The complementary regional myocardial uptake of ^{111}In-anti-TNC-Fab (radioactive half-life, 2.8 days) and ^{99m}Tc-MIBI (half-life, 6.0 hours) (Figure 3D, 3E, upper panels) was confirmed by autoradiography. Myocardial uptake of ^{111}In-anti-TNC-Fab was found more often in hearts with MI ($P = 0.035$) (Table II). The uptake of ^{111}In-anti-TNC-Fab was observed in the inferior myocardial region in one rat without ^{99m}Tc-MIBI defect.

Discussion

Our results demonstrate that the myocardial uptake of ^{111}In-anti-TNC-Fab was significantly higher in acute MI rats than in sham-operated rats. In autoradiography, high levels of radioactivity were clearly observed in the regions indicative of cardiac repair in acute MI rats. SPECT demonstrated the suitability of this tracer for *in vivo* imaging.

The expression of TNC was induced in interstitial fibroblasts of the border zone within 24 hours of permanent coronary ligation and it was reduced approx-

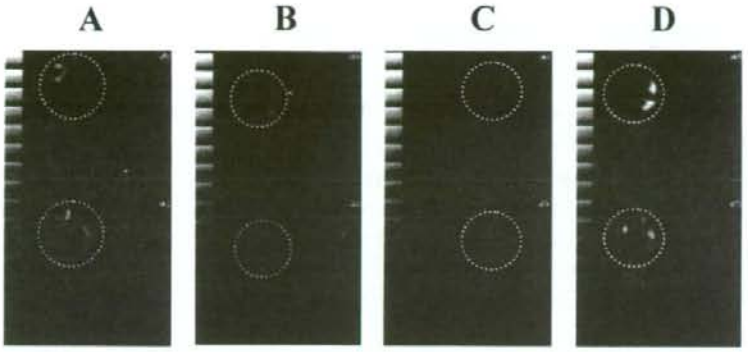

Figure 4. Examples of dual-isotope SPECT imaging after acute MI. Four examples of transverse dual-isotope SPECT images after acute MI (**A-D**). Upper panels show head side and lower ones show tail side. Red color indicates the uptake of ^{111}In-anti-TNC-Fab and green color, the uptake of ^{99m}Tc-MIBI. Myocardium is encircled by yellow broken lines.

imately 7 days after MI.[4] The 3 different time points after acute MI indicated that the peak uptake of ^{111}In-anti-TNC-Fab was within 7 days after MI in this study.

Localization of expression of TNC confirmed that the local uptake of ^{111}In-anti-TNC-Fab was similar to the immunohistochemical findings with the same antibody. To measure the effect of nonspecific deposition caused by low blood flow around ischemia, ^{111}In-nonspecific Fab was also investigated. The ratio of the radionuclide activity of infarcted area to noninfarcted area for ^{111}In-nonspecific Fab was 19% of the activity ratio for ^{111}In-anti-TNC-Fab. It has been reported that the nonspecific accumulation around the myocardial infarcted area should receive careful attention.[17] Here, no significant difference in activities was found between infarcted and noninfarcted areas after injection with ^{111}In-nonspecific Fab.

The Fab fragment specific for TNC was used in this study to reduce the total molecular weight of anti-TNC antibody. A radioactive tracer with a smaller molecule is expected to have a faster washout in blood and liver. Although Fab has neither reduced disulfide bonds nor a hinge region in Fab', Fab was able to bind to the chelating agent SCN-Bz-DTPA. The washout of anti-TNC Fab using SCN-Bz-DTPA was comparable to that of anti-TNC Fab' using EMCS-Bz-EDTA.[16]

Based on the notion of allowable nonspecific accumulation, *in vivo* SPECT imaging revealed regional uptake of ^{111}In-anti-TNC-Fab. It was demonstrated at sites complementary to ^{99m}Tc-MIBI uptake (Figure 3, upper panels, Figure 4A-D). One sham-operated rat with the uptake of ^{111}In-anti-TNC-Fab was probably caused by inflammation after the sham-operation. The liver uptake of ^{111}In-anti-TNC-Fab may also disturb myocardial evaluation. Therefore, careful observation

is needed at the myocardium adjacent to liver. However, an agreement between the existence of cardiac repair and MI certified that ^{111}In-anti-TNC-Fab reveals tissue repair caused by acute MI *in vivo*. In clinical situations after acute reperfusion therapy, ^{111}In-anti-TNC-Fab may be a reliable indicator to start intensive therapy for injured myocardium, since ^{99m}Tc-perfusion tracer is not able to differentiate stunned from necrotic myocardium within several days after MI.[18]

Various tracers for myocyte death imaging have already been developed. ^{111}In-antimyosin Fab imaging can be used to visualize active myocyte damage,[17,19] and thus has been employed in the diagnosis of MI.[20] ^{99m}Tc-annexin-V imaging has been reported for the noninvasive identification of apoptotic cell death in patients with acute MI[21] and heart transplantation.[22] ^{99m}Tc-labeled matrix metalloproteinase targeted radiotracer was introduced as a remodeling marker after MI.[23] Since there has been no method available for interstitial tissue imaging in patients, anti-TNC-Fab is superior to myocyte death imaging and is expected to depict cardiac tissue repair as an interstitial tissue tracer.

The human serum TNC level is reported to be a predictor of the progression of LV remodeling and prognosis.[5] Because serum TNC is synthesized and released by cardiac fibroblasts, local scintigraphic evaluation of TNC in myocardium may also be a predictor. The present animal study showed that the level of myocardial expression of TNC after acute MI was higher than the level of released TNC in the blood, and that radiolabeled anti-TNC-Fab might directly evaluate TNC kinetics in the myocardium. Scintigraphic analysis is thought to be of benefit by assessing myocardial TNC expression instead of serum TNC levels.

TNC expression is also induced in the injured myocardium in various heart diseases during the active stage.[24,25] We have previously demonstrated that TNC is expressed at the initial stage of myocarditis in an autoimmune mouse model before necrosis or inflammatory cell infiltration was histologically apparent.[11] Expression of TNC has also been observed in human coronary atherosclerotic plaque[26] and in restenotic neointima after angioplasty.[27] It loosens the strong adhesion of cardiomyocytes,[4] induces matrix metalloproteinases,[28] enhances the recruitment of myofibroblasts,[29] and possibly supports collagen fiber deposition.[30] Increased expression of TNC was observed early in relation to the onset of fibrosis and cardiac repair.[6] Therefore, *in vivo* imaging of TNC expression would be beneficial for understanding free cell rearrangement and tissue repair.

From a clinical aspect, monoclonal anti-TNC antibody has been injected into surgically-created resection cavities during brain tumor resections.[31] Although we must always be careful about anaphylactic shock against injected antibody, many clinical studies support the beneficial effects of anti-TNC antibody.

In conclusion, the present study verified that TNC antibody fragment can be

used to localize sites of cardiac repair in the heart by *ex vivo* and *in vivo* imaging. Although further studies will be necessary, radiolabeled anti-TNC-Fab may be useful for the noninvasive detection of cardiac repair after acute MI.

ACKNOWLEDGMENTS

We would like to thank Ms. Reiko Kobayashi and Ms. Emi Fujita for their technical assistance.

REFERENCES

1. Pfeffer MA, Braunwald E. Ventricular remodeling after myocardial infarction. Experimental observations and clinical implications. Circulation 1990; 81: 1161-72. (Review)
2. Tyagi SC. Proteinases and myocardial extracellular matrix turnover. Mol Cell Biochem 1997; 168: 1-12. (Review)
3. Imanaka-Yoshida K, Hiroe M, Yoshida T. Interaction between cell and extracellular matrix in heart disease: multiple roles of tenascin-C in tissue remodeling. Histol Histopathol 2004; 19: 517-25. (Review)
4. Imanaka-Yoshida K, Hiroe M, Nishikawa T, *et al.* Tenascin-C modulates adhesion of cardiomyocytes to extracellular matrix during tissue remodeling after myocardial infarction. Lab Invest 2001; 81: 1015-24.
5. Sato A, Aonuma K, Imanaka-Yoshida K, *et al.* Serum tenascin-C might be a novel predictor of left ventricular remodeling and prognosis after acute myocardial infarction. J Am Coll Cardiol 2006; 47: 2319-25.
6. Chaulet H, Lin F, Guo J, *et al.* Sustained augmentation of cardiac alpha1A-adrenergic drive results in pathological remodeling with contractile dysfunction, progressive fibrosis and reactivation of matricellular protein genes. J Mol Cell Cardiol 2006; 40: 540-52.
7. Reynolds JC, Del Vecchio S, Sakahara H, *et al.* Anti-murine antibody response to mouse monoclonal antibodies: clinical findings and implications. Int J Rad Appl Instrum B 1989; 16: 121-5.
8. Seccamani E, Tattanelli M, Mariani M, Spranzi E, Scassellati GA, Siccardi AG. A simple qualitative determination of human antibodies to murine immunoglobulins (HAMA) in serum samples. Int J Rad Appl Instrum B 1989; 16: 167-70.
9. Saga Y, Yagi T, Ikawa Y, Sakakura T, Aizawa S. Mice develop normally without tenascin. Genes Dev 1992; 6: 1821-31.
10. Aukhil I, Slemp CC, Lightner VA, Nishimura K, Briscoe G, Erickson HP. Purification of hexabrachion (tenascin) from cell culture conditioned medium, and separation from a cell adhesion factor. Matrix 1990; 10: 98-111.
11. Imanaka-Yoshida K, Hiroe M, Yasutomi Y, *et al.* Tenascin-C is a useful marker for disease activity in myocarditis. J Pathol 2002; 197: 388-94.
12. Cummins CH, Rutter EW Jr, Fordyce WA. A convenient synthesis of bifunctional chelating agents based on diethylenetriaminepentaacetic acid and their coordination chemistry with yttrium (III). Bioconjug Chem 1991; 2: 180-6.
13. Arano Y, Mukai T, Uezono T, *et al.* A biological method to evaluate bifunctional chelating agents to label antibodies with metallic radionuclides. J Nucl Med 1994; 35: 890-8.
14. Arano Y, Uezono T, Akizawa H, *et al.* Reassessment of diethylenetriaminepentaacetic acid (DTPA) as a chelating agent for indium-111 labeling of polypeptides using a newly synthesized monoreactive DTPA derivative. J Med Chem 1996; 39: 3451-60.
15. Arano Y, Wakisaka K, Mukai T, *et al.* Stability of a metabolizable ester bond in radioimmunoconjugates. Nucl Med Biol 1996; 23: 129-36.
16. Sato M, Toyozaki T, Odaka K, *et al.* Detection of experimental autoimmune myocarditis in rats by 111In monoclonal antibody specific for tenascin-C. Circulation 2002; 106: 1397-02.

17. Khaw BA, Petrov A, Narula J. Complementary roles of antibody affinity and specificity for in vivo diagnostic cardiovascular targeting: how specific is antimyosin for irreversible myocardial damage? J Nucl Cardiol 1999; 6: 316-23.
18. Tanaka R, Nakamura T. Time course evaluation of myocardial perfusion after reperfusion therapy by 99mTc-tetrofosmin SPECT in patients with acute myocardial infarction. J Nucl Med 2001; 42: 1351-8.
19. Puig M, Ballester M, Matias-Guiu X, *et al*. Burden of myocardial damage in cardiac allograft rejection: scintigraphic evidence of myocardial injury and histologic evidence of myocyte necrosis and apoptosis. J Nucl Cardiol 2000; 7: 132-9.
20. Sarda L, Colin P, Boccara F, *et al*. Myocarditis in patients with clinical presentation of myocardial infarction and normal coronary angiograms. J Am Coll Cardiol 2001; 37: 786-92.
21. Hofstra L, Liem IH, Dumont EA, *et al*. Visualization of cell death in vivo in patients with acute myocardial infarction. Lancet 2000; 356: 209-12.
22. Narula J, Acio ER, Narula N, *et al*. Annexin-V imaging for noninvasive detection of cardiac allograft rejection. Nat Med 2001; 7: 1347-52.
23. Su H, Spinale FG, Dobrucki LW, *et al*. Noninvasive targeted imaging of matrix metalloproteinase activation in a murine model of postinfarction remodeling. Circulation 2005; 112: 3157-67.
24. Willems IE, Arends JW, Daemen MJ. Tenascin and fibronectin expression in healing human myocardial scars. J Pathol 1996; 179: 321-5.
25. Frangogiannis NG, Shimoni S, Chang SM, *et al*. Active interstitial remodeling: an important process in the hibernating human myocardium. J Am Coll Cardiol 2002; 39: 1468-74.
26. Wallner K, Li C, Shah PK, *et al*. Tenascin-C is expressed in macrophage-rich human coronary atherosclerotic plaque. Circulation 1999; 99: 1284-9.
27. Imanaka-Yoshida K, Matsuura R, Isaka N, Nakano T, Sakakura T, Yoshida T. Serial extracellular matrix changes in neointimal lesions of human coronary artery after percutaneous transluminal coronary angioplasty: clinical significance of early tenascin-C expression. Virchows Arch 2001; 439: 185-90.
28. Kalembeyi I, Inada H, Nishiura R, Imanaka-Yoshida K, Sakakura T, Yoshida T. Tenascin-C upregulates matrix metalloproteinase-9 in breast cancer cells: direct and synergistic effects with transforming growth factor beta1. Int J Cancer 2003; 105: 53-60.
29. Tamaoki M, Imanaka-Yoshida K, Yokoyama K, *et al*. Tenascin-C regulates recruitment of myofibroblasts during tissue repair after myocardial injury. Am J Pathol 2005; 167: 71-80.
30. Toma N, Imanaka-Yoshida K, Takeuchi T, *et al*. Tenascin-C-coated platinum coils for acceleration of organization of cavities and reduction of lumen size in a rat aneurysm model. J Neurosurg 2005; 103: 681-6.
31. McLendon RE, Akabani G, Friedman HS, *et al*. Tumor resection cavity administered iodine-131-labeled antitenascin 81C6 radioimmunotherapy in patients with malignant glioma: neuropathology aspects. Nucl Med Biol 2007; 34: 405-13.

Circ J 2009; **73:** 158–161

Mutational Analysis of Fukutin Gene in Dilated Cardiomyopathy and Hypertrophic Cardiomyopathy

Takuro Arimura, DVM*; Yukiko K. Hayashi, MD**; Terumi Murakami, MD**; Yasushi Oya, MD†; Sayaka Funabe, MD††; Eri Arikawa-Hirasawa, MD††; Nobutaka Hattori, MD††; Ichizo Nishino, MD**; Akinori Kimura, MD*,‡

Background Mutations in *FKTN* encoding for fukutin cause Fukuyama-type congenital muscular dystrophy characterized by severe muscle wasting and hypotonia with mental retardation. Fukuyama-type congenital muscular dystrophy is a recessive genetic trait. *FKTN* mutations in patients with dilated cardiomyopathy (DCM) have been investigated by our research group. The patients showed hyper-CKemia with mild or no muscle weakness and without mental retardation, suggesting that the clinical spectrum of *FKTN* mutations are wider than previously thought. The current study was designed to further explore the association of *FKTN* mutations with DCM or hypertrophic cardiomyopathy (HCM).

Methods and Results A total of 172 patients with DCM, 144 patients with familial HCM and 384 control individuals were analyzed for *FKTN* mutations. There was a DCM patient who was a compound heterozygote of a 3-kb insertion mutation and a missense mutation Cys101Phe. The patient showed hyper-CKemia with mild muscle involvement and no brain involvement. In contrast, 2 other DCM patients and 3 controls were heterozygous for the insertion mutation and normal allele, showing that the heterozygous insertion mutation itself was not associated with DCM. No mutation was found in the HCM patients.

Conclusions These observations indicated that the compound heterozygous *FKTN* mutation was a rare cause of DCM. Hyper-CKemia might be indicative of *FKTN* mutation in DCM. (*Circ J* 2009; **73:** 158–161)

Key Words: Cardiomyopathy; Genes; Genetics; Muscles

Idiopathic cardiomyopathy (ICM), which is mainly classified into 2 clinical phenotypes; hypertrophic cardiomyopathy (HCM) and dilated cardiomyopathy (DCM), is a primary heart muscle disorder caused by functional abnormalities in the cardiomyocytes and a major cause of sudden cardiac death and progressive heart failure[1] Although the etiology of ICM has not been completely elucidated, recent molecular genetic studies have shown that ICM can be caused by a variety of genetic abnormalities[1] Inheritance of familial HCM is usually autosomal dominant, whereas that of familial DCM is autosomal dominant, autosomal recessive, or X-linked recessive, ie, various type of disease inheritance can be found in DCM cases[2,3] It also should be noted that causative gene mutations could be found not only in familial cases but also in sporadic cases, indicating that the absence of family history cannot exclude a possibility of causative gene mutation in ICM cases[3] In addition, mutations in muscular dystrophy-causing genes might also lead to ICM phenotype, as exemplified that titin/connectin gene (*TTN*) mutations were found in patients with HCM[4] DCM[5] or tibial musclular dystrophy and limb-girdle type muscular dystrophy (LGMD)[6] and that Tcap gene (*TCAP*) mutations were found in HCM and DCM[7] as well as in LGMD[8] These observations indicate that there is an etiological overlap between ICM, and the skeletal muscle disorders[9]

Mutations in *FKTN* encoding for fukutin cause Fukuyama-type congenital muscular dystrophy (FCMD; MIM253800), the second most common muscular dystrophy in Japan after Duchenne muscular dystrophy. FCMD is an autosomal recessive disease manifested with severe muscle wasting and mental retardation[10,11] The majority of the FCMD patients were homozygous for a 3-kb insertion in the 3' non-coding region of *FKTN*, whereas a small population of FCMD patients were compound heterozygotes of the 3-kb insertion and a missense mutation[12,13] In addition, we recently identified compound heterozygotes of the insertion and a missense mutation in 2 sibling cases and 2 sporadic cases of DCM, who manifested with minimal muscle weakness and elevated serum creatine kinase (CK) concentration, hyper-CKemia, but not mental retardation[14] However, it remains unknown whether *FKTN* mutation can be associated with ICM not accompanied by signs of muscular dystrophy and in which type of ICM patients who should be examined for *FKTN* mutations as a disease-causing gene.

In the present study, we searched for *FKTN* mutations in a large panel of patients with DCM or HCM. We found a compound heterozygote of *FKTN* mutations in 1 out of 172 DCM patients, who also had mild muscular dystrophy and hyper-CKemia.

(Received July 24, 2008; revised manuscript received August 12, 2008; accepted August 21, 2008; released online November 17, 2008)

**Department of Molecular Pathogenesis, Medical Research Institute, Tokyo Medical and Dental University, **Department of Neuromuscular Research, National Institute of Neuroscience, National Center of Neurology and Psychiatry (NCNP), †Department of Neurology, National Center Hospital of Neurology and Psychiatry, NCNP, ††Department of Neurology, Juntendo University School of Medicine and ‡Laboratory of Genome Diversity, School of Biomedical Science, Tokyo Medical and Dental University, Tokyo, Japan*

Mailing address: Akinori Kimura, MD, Department of Molecular Pathogenesis, Medical Research Institute, Tokyo Medical and Dental University, 1-5-45 Yushima, Bunkyo-ku, Tokyo 113-8510, Japan. E-mail: akitis@mri.tmd.ac.jp

Methods

Study Population

We studied 172 genetically unrelated Japanese patients with DCM and 144 patients with familial HCM. Among the DCM patents, family history was not found in 100 patients (sporadic cases), whereas apparent family history was found in 72 patients; 4 were probands of sibling cases (possible autosomal recessive cases) and 68 patients were probands of DCM families, in which disease was inherited as a autosomal dominant genetic trait. In addition, family history consistent with autosomal dominant inheritance was found in all HCM patients. The patients were diagnosed based on medical history, physical examination, 12-lead electrocardiogram (ECG), echocardiography, and other special tests if necessary. Diagnostic criteria for DCM and HCM were described previously[7,15] These patients had been investigated for mutations in the known disease genes for ICM, such as sarcomere genes and Z-disc component genes[3] and no disease-causing mutations were identified. All patients showed no sign of brain involvement, ie, typical FCMD cases were clinically excluded. Control subjects were 384 unrelated healthy Japanese individuals selected at random. After acquiring informed consent, blood samples were obtained from each participant. The research protocol was approved by the Ethics Review Committee of Medical Research Institute, Tokyo Medical and Dental University and that of National Institute of Neuroscience, National Center of Neurology and Psychiatry.

Mutational Analysis of FKTN in ICM

Genomic DNA extracted from peripheral blood was subjected to polymerase chain reaction (PCR). To detect the 3-kb insertion in *FKTN*, we carried out PCR in all participants using 2 primer sets as described previously[14,16] Entire exons and their flanking regions of *FKTN* were directly sequenced on both strands by using an ABI PRISM 3100 automated sequencer (PE Applied Biosystems Foster City, CA, USA) as reported previously[14]

Immunohistochemical Analysis

Monoclonal anti-α-DG (VIA4-1, Upstate Biotechnology, Lake Placid, NY, USA) and monoclonal anti-β-DG (43DAG1/8D5, Novocastra Laboratories, Newcastle upon Tyne, UK) were used for immunostaining of biopsied skeletal muscle samples as described previously[14]

Results

The 3-kb insertion mutation was searched in 172 DCM patients and 144 HCM patients. We found that 3 patients (all were sporadic DCM cases) carried the insertion mutation in the heterozygous state. This 3-kb insertion was not detected in other patients, but was identified in 3 out of 384 controls. We then sequenced all exons and adjacent introns of *FKTN* in the 3 sporadic DCM patients carrying the 3-kb insertion (**Fig 1A**) and found a missense mutation (c.302G>T, p.Cys101Phe) in one case (**Fig 1B**), suggesting that this patient was a compound heterozygote of *FKTN* mutations.

The patient was a 19-year-old female who manifested with exertional dyspnea and mild muscular weakness at neck and proximal extremities along with bilateral calf hypertrophy. She had shown hyper-CKemia (6,570IU/L) without any muscle symptoms from the age of 17 years. Since then, she was followed up by physicians as a result of

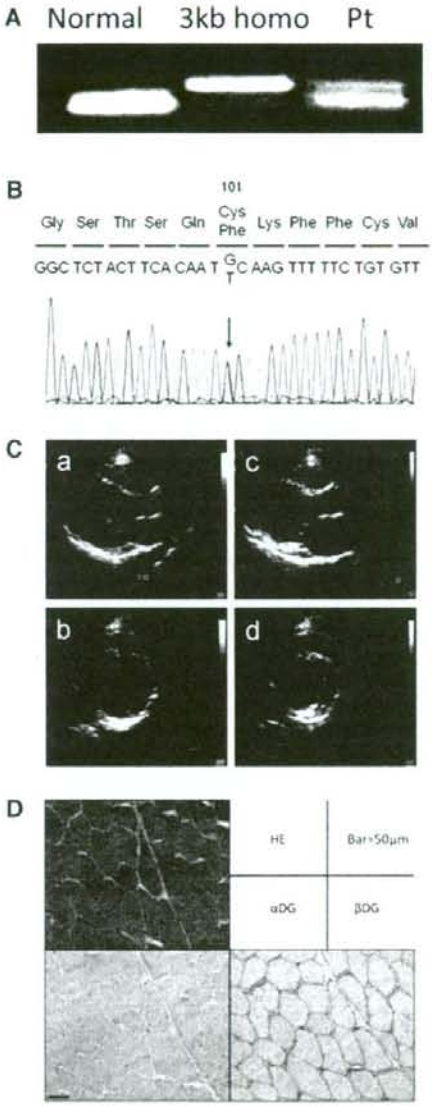

Fig 1. Gene and histochemical analyses of the dilated cardiomyopathy (DCM) patient carrying the *FKTN* mutation. (**A**) Detection of 3-kb insertion. Left, normal individual without mutation; middle, Fukuyama-type congenital muscular dystrophy patient carrying homozygous 3-kb insertion; right, the DCM patient with *FKTN* mutation. The patient showed both normal and insertion bands. (**B**) Direct sequencing data from the DCM patient. Polymerase chain reaction products containing exon 4 of *FKTN* gene from the patient were directly sequenced. Nucleotide sequences are shown along with predicted amino acid sequences. An arrowhead indicates the mutation resulting in TGC (Cys) to TTC (Phe) change. (**C**) Echocardiography of the patient. Endodiastolic (**a, b**) and endosystolic (**c, d**) data for sagital (**a, c**) and vertical (**b, d**) views showing left ventricular dilation. (**D**) Hematoxylin and eosin staining (HE) and immunohistochemical analysis. On HE, only mild variation in fiber size was found. Immunohistochemical analysis using a monoclonal antibody VIA4-1 that recognizes heavily-glycosylated form of α-dystroglycan (αDG), showed reduced sarcolemmal staining, whereas the staining of β-dystroglycan (βDG) using monoclonal antibody 43DAG1/8D5 showed no abnormality. Bar=50 μm.

the hyper-CKemia of unknown etiology. Diffuse left ventricular hypokinesis with left ventricular ejection fraction (LVEF) of 38% was observed at the age of 18 years, along with diffuse muscle atrophy and mild necrosis-regeneration process in biceps brachii muscle biopsy. She felt excertional dyspnea from the age of 18 years and when she was 19 years old, her ECG showed incomplete right bundle branch block, and her echocardiogram showed systolic dysfunction with ventricular dilatation (LVEF, 41%; left ventricular end-diastolic diameter, 53 mm; left ventricular end-systolic diameter, 43 mm; fractional shortening, 20%), whereas no ventricular hypertrophy was observed (inter ventricular septum, 6 mm; posterior wall, 7 mm). Biochemical analysis showed that she had hyper-CKemia (2,485 IU/L). Immunohistochemical analysis of biopsied muscle sample showed marked decrease of α-dystroglycan staining, whereas distribution and expression of β-dystroglycan was not changed (**Fig 1B**). This finding was consistent with *FKTN* mutations[14] albeit that no family history of DCM or muscle disease was evident with her. From these observations, she was finally diagnosed as LGMD manifested with mild DCM phenotype.

In addition, we sequenced the entire coding regions and adjacent introns of *FKTN* from 72 patients with familial DCM (4 consistent with recessive inheritance and 68 with dominant inheritance). The sequencing analyses showed 2 variations, 1 non-synonymous change in exon 5 (c.608G > A, p.Arg203Gln) and 1 synonymous change in exon 8 (c.1026C > A, p.Leu342Leu), in several patients. However, both variations were reported to be polymorphisms in the SNP database (rs34787999 and rs17309806, respectively), suggesting that these were polymorphisms not related with DCM.

Discussion

The 3-kb insertion into the 3'-untranslated region of the *FKTN*, which has been derived from a single ancestral founder and causes a significant reduction of *FKTN* mRNA, could cause FCMD in homozygous states or in compound heterozygous states with another point mutation[12,13] FCMD is one of the most severe congenital muscular dystrophy in combination with brain malformation, principally cerebral and cerebellar cortical dysplasia[10,11] In contrast to the severely affected skeletal muscle, cardiac muscle involvement is quite rare in FCMD patients. However, we recently showed that the compound heterozygous mutations could also be associated with DCM accompanied by minimal limb girdle muscle involvement and normal intelligence[14] These observations implied the wide phenotypic spectrum of the *FKTN* mutations. In the current study, we identified a patient carrying the 3-kb insertion and a missense mutation, who manifested with DCM and mild skeletal muscle phenotype. Clinical phenotype of the patient in this study was similar to those reported previously[14] further supporting that the compound heterozygous mutation was associated with DCM. Because we have not examined her parents for the *FKTN* mutations, we could not formally exclude a possibility that these 2 mutations were in *trans* and not in *cis*. However, if the mutations were in *cis*, this patient should have one normal allele and the other non-expressing allele due to the 3-kb insertion, which is in a similar situation as the heterozygote of the 3-kb mutation; the situation not causing any disease phenotypes as discussed below.

The 3-kb insertion was also found in 2 other sporadic DCM cases, but these patients did not carry any additional *FKTN* mutations nor did they show hyper-CKemia, indicating that heterozygote of the insertion mutation and normal allele did not manifest with cardiomyopathy or muscle diseases. In addition, we identified 3 heterozygous carriers of the 3-kb insertion in 384 Japanese controls (0.78%), and this carrier frequency was similar to those previously reported by 2 other groups (6 in 676; 0.89%[16] and 15 in 2,814; 0.53%[17]). In this study, we investigated familial HCM patients for *FKTN* mutations even though the disease was inherited as an autosomal dominant trait as in the most cases of familial DCM. Because mutations in the muscular dystrophy genes such as *TTN* and *TCAP* cause skeletal muscle disease as the autosomal recessive trait and cardiomyopathy (HCM or DCM) as the autosomal dominant trait, we had not been able to exclude a possibility of *FKTN* mutations in autosomal dominant cases. However, no *FKTN* mutation was found in the patients with familial HCM as in familial DCM, examined in this study. These observations suggest that *FKTN* mutations should be considered as a cause of DCM, albeit not a major cause, especially in the sporadic cases or sibling cases.

What was the characteristic feature of DCM caused by *FKTN* mutations? The patient carrying the causative *FKTN* mutations showed hyper-CKemia before manifesting with cardiomyopathy and skeletal muscle symptoms. All the patients carrying the compound heterozygous mutations in the previous study had elevated serum CK concentrations, although they showed no or minimal skeletal muscle phenotypes[14] The hyper-CKemia can also be found in the patients carrying *FKTN* mutations affected with FCMD[18] or LGMD[19,20] These observations are in good agreement with the association between the *FKTN* mutations and hyper-CKemia. In our cohort of DCM patients, we identified disease-causing mutations in 4 sporadic DCM patients who showed continuously hyper-CKemia. One was the patient carrying the *FKTN* mutations reported here, whereas the other 3 patients had abnormalities in the dystrophin gene (DMD) with a deletion of exon 3, exon 44, or exons 45–51. The DCM patients with DMD mutations showed elevated serum CK concentrations of approximately 500–1,000 IU/L. The finding was in part consistent with that DCM patients carrying DMD mutations were reported to show hyper-CKemia even though they had no or minimal symptoms of muscle involvement[21,22] These observations suggested that hyper-CKemia in patients with DCM might be an indicative sign of *FKTN* or *DMD* mutations.

In summary, we have investigated *FKTN* mutations in a large panel of patients with DCM or HCM and found that a sporadic DCM case with hyper-CKemia was a compound heterozygote of *FKTN* mutations.

Acknowledgements

We are grateful to Drs H. Toshima, H. Nishi, K. Matsuyama, H. Kagiyama, T. Sakamoto, K. Kawai, K. Kawamura, R. Kusukawa, M. Nagano, Y. Nimura, R. Okada, T. Sugimoto, H. Tanaka, H. Yasuda, F. Numano, K. Fukuda, S. Ogawa, A. Matsumori, S. Sasayama, R. Nagai, and Y. Yazaki for their contributions in clinical evaluation and blood sampling from patients with DCM. We also thank Dr M. Yanokura, Ms M. Emura and Ms A. Nishimura for their technical assistance. This work was supported in part by Grant-in-aids from the Ministry of Education, Culture, Sports, Science and Technology, Japan; Grant-in-Aids for Scientific Research from the Japan Society for the Promotion of Science, Research on Psychiatric and Neurological Diseases and Mental Health from Health and Labor Sciences Research Grants, and research grants for Idiopathic Cardiomyopathy and for Nervous and Mental Disorders from the Ministry of Health, Labour and Welfare, Japan, Program for Promotion of Fundamental Studies in Health Sciences of the National Institute of Biomedical

Innovation, and Association Française contre les Myopathies.

References

1. Maron BJ, Towbin JA, Thiene G, Antzelevitch C, Corrado D, Arnett D, et al. Contemporary definitions and classification of the cardiomyopathies: An American Heart Association Scientific Statement from the Council on Clinical Cardiology, Heart Failure and Transplantation Committee; Quality of Care and Outcomes Research and Functional Genomics and Translational Biology Interdisciplinary Working Groups; and Council on Epidemiology and Prevention. *Circulation* 2006; **113:** 1807–1816.
2. Michels VV, Moll PP, Miller FA, Tajik AJ, Chu JS, Driscoll DJ, et al. The frequency of familial dilated cardiomyopathy in a series of patients with idiopathic dilated cardiomyopathy. *N Engl J Med* 1992; **326:** 77–82.
3. Kimura A. Molecular etiology and pathogenesis of hereditary cardiomyopathy. *Circ J* 2008; **72**(Suppl): A-38–A-48.
4. Satoh M, Takahashi M, Sakamoto T, Hiroe M, Marumo F, Kimura A, et al. Structural analysis of the titin gene in hypertrophic cardiomyopathy: Identification of a novel disease gene. *Biochem Biophys Res Commun* 1999; **262:** 411–417.
5. Itoh-Satoh M, Hayashi T, Nishi H, Koga Y, Arimura T, Koyanagi T, et al. Titin mutations as the molecular basis for dilated cardiomyopathy. *Biochem Biophys Res Commun* 2002; **291:** 385–393.
6. Hackman P, Vihola A, Haravuori H, Marchand S, Sarparanta J, De Seze J, et al. Tibial muscular dystrophy is a titinopathy caused by mutations in TTN, the gene encoding the giant skeletal-muscle protein titin. *Am J Hum Genet* 2002; **71:** 492–500.
7. Hayashi T, Arimura T, Itoh-Satoh M, Ueda K, Hohda S, Inagaki N, et al. Tcap gene mutations in hypertrophic cardiomyopathy and dilated cardiomyopathy. *J Am Coll Cardiol* 2004; **44:** 2192–2201.
8. Moreira ES, Wiltshire TJ, Faulkner G, Nilforoushan A, Vainzof M, Suzuki OT, et al. Limb-girdle muscular dystrophy type 2G is caused by mutations in the gene encoding the sarcomeric protein telethonin. *Nature Genet* 2000; **24:** 163–166.
9. McNally E, Allikian M, Wheeler MT, Mislow JM, Heydemann A. Cytoskeletal defects in cardiomyopathy. *J Mol Cell Cardiol* 2003; **35:** 231–241.
10. Fukuyama Y, Osawa M, Suzuki H. Congenital progressive muscular dystrophy of the Fukuyama type–clinical, genetic and pathological considerations. *Brain Dev* 1981; **3:** 1–29.
11. Kondo-Iida E, Saito K, Tanaka H, Tsuji S, Ishihara T, Osawa M, et al. Molecular genetic evidence of clinical heterogeneity in Fukuyama-type congenital muscular dystrophy. *Hum Genet* 1997; **99:** 427–432.
12. Kobayashi K, Nakahori Y, Miyake M, Matsumura K, Kondo-Iida E, Nomura Y, et al. An ancient retrotransposal insertion causes Fukuyama-type congenital muscular dystrophy. *Nature* 1998; **394:** 388–392.
13. Kondo-Iida E, Kobayashi K, Watanabe M, Sasaki J, Kumagai T, Koide H, et al. Novel mutations and genotype-phenotype relationships in 107 families with Fukuyama-type congenital muscular dystrophy (FCMD). *Hum Mol Genet* 1999; **8:** 2303–2309.
14. Murakami T, Hayashi YK, Noguchi S, Ogawa M, Nonaka I, Tanabe Y, et al. Fukutin gene mutations cause dilated cardiomyopathy with minimal muscle weakness. *Ann Neurol* 2006; **60:** 597–602.
15. Arimura T, Hayashi T, Terada H, Lee SY, Zhou Q, Takahashi M, et al. A Cypher/ZASP mutation associated with dilated cardiomyopathy alters the binding affinity to protein kinase C. *J Biol Chem* 2004; **279:** 6746–6752.
16. Kato R, Kawamura J, Sugawara H, Niikawa N, Matsumoto N. A rapid diagnostic method for a retrotransposal insertional mutation into the FCMD gene in Japanese patients with Fukuyama congenital muscular dystrophy. *Am J Med Genet A* 2004; **127:** 54–57.
17. Watanabe M, Kobayashi K, Jin F, Park KS, Yamada T, Tokunaga K, et al. Founder SVA retrotransposal insertion in Fukuyama-type congenital muscular dystrophy and its origin in Japanese and Northeast Asian populations. *Am J Med Genet A* 2005; **138:** 344–348.
18. Silan F, Yoshioka M, Kobayashi K, Simsek E, Tunc M, Alper M, et al. A new mutation of the fukutin gene in a non-Japanese patient. *Ann Neurol* 2003; **53:** 392–396.
19. Godfrey C, Escolar D, Brockington M, Clement EM, Mein R, Jimenez-Mallebrera C, et al. Fukutin gene mutations in steroid-responsive limb girdle muscular dystrophy. *Ann Neurol* 2006; **60:** 603–610.
20. Lin YC, Murakami T, Hayashi YK, Nishino I, Nonaka I, Yuo CY, et al. A novel FKRP gene mutation in a Taiwanese patient with limb-girdle muscular dystrophy 2I. *Brain Dev* 2007; **29:** 234–238.
21. Mirabella M, Servidei S, Manfredi G, Ricci E, Frustaci A, Bertini E, et al. Cardiomyopathy may be the only clinical manifestation in female carriers of Duchenne muscular dystrophy. *Neurology* 1993; **43:** 2342–2345.
22. Feng J, Yan J, Buzin CH, Towbin JA, Sommer SS. Mutations in the dystrophin gene are associated with sporadic dilated cardiomyopathy. *Mol Genet Metab* 2002; **77:** 119–126.

Local Tenomodulin Absence, Angiogenesis, and Matrix Metalloproteinase Activation Are Associated With the Rupture of the Chordae Tendineae Cordis

Naritaka Kimura, MD; Chisa Shukunami, DDS, PhD; Daihiko Hakuno, MD, PhD; Masatoyo Yoshioka, MD, PhD; Shigenori Miura, PhD; Denitsa Docheva, PhD; Tokuhiro Kimura, MD; Yasunori Okada, MD, PhD; Goki Matsumura, MD, PhD; Toshiharu Shin'oka, MD, PhD; Ryohei Yozu, MD, PhD; Junjiro Kobayashi, MD, PhD; Hatsue Ishibashi-Ueda, MD, PhD; Yuji Hiraki, PhD; Keiichi Fukuda, MD, PhD

Background—Rupture of the chordae tendineae cordis (CTC) is a well-known cause of mitral regurgitation. Despite its importance, the mechanisms by which the CTC is protected and the cause of its rupture remain unknown. CTC is an avascular tissue. We investigated the molecular mechanisms underlying the avascularity of CTC and the correlation between avascularity and CTC rupture.

Methods and Results—We found that tenomodulin, which is a recently isolated antiangiogenic factor, was expressed abundantly in the elastin-rich subendothelial outer layer of normal rodent, porcine, canine, and human CTC. Conditioned medium from cultured CTC interstitial cells strongly inhibited tube formation and mobilization of endothelial cells; these effects were partially inhibited by small-interfering RNA against tenomodulin. The immunohistochemical analysis was performed on 12 normal and 16 ruptured CTC obtained from the autopsy or surgical specimen. Interestingly, tenomodulin was locally absent in the ruptured areas of CTC, where abnormal vessel formation, strong expression of vascular endothelial growth factor-A and matrix metalloproteinases, and infiltration of inflammatory cells were observed, but not in the normal or nonruptured area. In anesthetized open-chest dogs, the tenomodulin layer of tricuspid CTC was surgically filed, and immunohistological analysis was performed after several months. This intervention gradually caused angiogenesis and expression of vascular endothelial growth factor-A and matrix metalloproteinases in the core collagen layer in a time-dependent manner.

Conclusions—These findings provide evidence that tenomodulin is expressed universally in normal CTC in a concentric pattern and that local absence of tenomodulin, angiogenesis, and matrix metalloproteinase activation are associated with CTC rupture. (***Circulation.*** **2008;118:1737-1747.)**

Key Words: angiogenesis ■ chordae tendineae cordis ■ metalloproteinases ■ tenomodulin ■ valves

Although the heart is a vascularized organ, the cardiac valves and chordae tendineae cordis (CTC) are avascular tissues.[1] This avascularity is abrogated in several valvular heart diseases (VHDs).[2–4] Chondromodulin-I, which is an antiangiogenic factor isolated from bovine cartilage,[5–8] is also expressed in the eye and is critically involved in the maintenance. Recently, we have reported that chondromodulin-I was abundantly expressed by the valvular interstitial cells in normal cardiac valves.[9] Gene targeting of chondromodulin-I resulted in enhanced vascular endothelial growth factor (VEGF)-A expression, lipid deposition, and calcification in the cardiac valves of aged mice. In human VHDs, including infective endocarditis, rheumatic heart disease, and atherosclerosis, VEGF-A expression, neovascularization, and calcification were observed in areas of chondromodulin-I downregulation. These findings provide evidence that chondromodulin-I plays a pivotal role in maintaining normal valvular function by preventing angiogenesis that might lead to VHD.

Received March 15, 2008; accepted July 23, 2008.

From the Departments of Regenerative Medicine and Advanced Cardiac Therapeutics (N.K., D.H., M.Y., K.F.), Cardiovascular Surgery (N.K., R.Y.), and Pathology (T.K., Y.O.), Keio University School of Medicine, Tokyo, Japan; Department of Cellular Differentiation, Institute for Frontier Medical Sciences, Kyoto University, Kyoto, Japan (C.S., S.M., Y.H.); Department of Molecular Medicine, Max Planck Institute of Biochemistry, Martinstried, Germany (D.D.); Department of Cardiovascular Surgery, Heart Institute of Japan, Tokyo Women's Medical University, Tokyo, Japan (G.M., T.S.); and Departments of Cardiovascular Surgery (J.K.) and Pathology (H.I.-U.), National Cardiovascular Center Hospital, Osaka, Japan.

The online-only Data Supplement is available with this article at http://circ.ahajournals.org/cgi/content/full/CIRCULATIONAHA.108.780031/DC1.

GenBank accession number: murine tenomodulin, NM_022322.

Correspondence to Keiichi Fukuda, MD, PhD, 35 Shinanomachi, Shinjuku, Tokyo 160-8582, Japan. E-mail kfukuda@sc.itc.keio.ac.jp

Circulation **is available at http://circ.ahajournals.org** **DOI: 10.1161/CIRCULATIONAHA.108.780031**

Editorial p 1694
Clinical Perspective p 1747

Rupture of the CTC is a well-known cause of mitral regurgitation. To elucidate the molecular mechanism, we investigated the expression of chondromodulin-I in the CTC. Unexpectedly, both normal and ruptured CTC lacked expression of chondromodulin-I, suggesting that the mechanism underlying the avascularity or protective function of the CTC differed from that operating in cardiac valves, even though the cardiac valves and CTC lie in proximity to each other and have a similar avascular appearance. The atrioventricular valve leaflets and CTC comprise diverse cell lineages and highly organized matrices that are populated by cartilage[10,11] and tendon[12,13] cell types, respectively. The cartilage cell markers aggrecan and Sox9 are observed in valvular leaflets during embryogenic valvulogenesis, whereas the tendon-associated genes *Scleraxis* and *Tenascin* are expressed in the CTC.[14,15] On the basis of these observations and our previous findings regarding chondromodulin-I in cardiac valves,[9] we speculated that CTC avascularity might be related to the avascular properties of tendon rather than those of cartilage.

Recently, we isolated tenomodulin, which is a novel chondromodulin-I–related gene with 33% amino acid identity. Tenomodulin is a 317–amino acid glycoprotein found in hypovascular tissues, such as tendons, ligaments, the epimysium, and eyes.[16–19] Tenomodulin contains BRICHOS and cysteine-rich domains[20] and has antiangiogenic activities. It is processed in vivo in certain tissues, and the proteolytically cleaved, 16-kDa C-terminal domain promotes tenocyte proliferation.[21,22] In the present study, we investigated whether tenomodulin is expressed in the CTC and its potential involvement in CTC avascularity. We also investigated the cause of the rupture of CTC by comparing the normal and ruptured CTC from the viewpoint of angiogenesis and the involvement of tenomodulin.

Methods

Animals

Wild-type ICR mice were purchased from Japan CLEA (Tokyo, Japan). Japanese White rabbits were purchased from Sankyo Laboratory Service Corporation (Tokyo, Japan). Porcine eyes and hearts were purchased from a public slaughterhouse (Tokyo, Japan). Adult beagle dogs were purchased from NARC Corporation (Chiba, Japan). All experimental procedures and protocols were approved by the animal care and use committees of Keio University and conformed to the National Institutes of Health *Guidelines for the Care and Use of Laboratory Animals*.

Reverse Transcription Polymerase Chain Reaction

Total RNA was isolated with the use of Trizol reagent (GIBCO-BRL) and treated with DNase I (Roche). Reverse transcription polymerase chain reaction (RT-PCR) was performed as described previously[9] with the following primers: murine tenomodulin, 5′-AGAATGAGCAATGGGTGGTC-3′ (forward), 3′-CTCGACCTCCTTGGTAGCAG-5′ (reverse); murine GAPDH, 5′-TTCAACGGCACAGTCAAGG-3′ (forward), 3′-CATGGACTGTGGTCATGAG-5′ (reverse); porcine tenomodulin, 5′-GGTGGTCCCTCAAGTGAAAG-3′ (forward), 3′-CTCGTCCTCCTTGGTAGCAG-5′ (reverse); porcine GAPDH, 5′-TGATGACATCAAGAAGGTGGTGAAG-3′ (forward), 3′-TCCTTGGAGGCCATGTGGACCAT-5′ (reverse).

Immunohistochemical and Immunofluorescence Staining

Conceived or nonconceived adult mouse hearts were perfused from the apex with phosphate-buffered saline, perfusion-fixed with 4% paraformaldehyde in phosphate-buffered saline, and used for immunostaining as described previously.[23] The CTC were dissected, immersion-fixed overnight at 4°C in 4% paraformaldehyde, and then embedded in paraffin. Before application of the primary antibodies, paraffin was removed from the sections in xylene, and the sections were heated in a microwave oven in 10 mmol/L citrate buffer solution (pH 6.0) (Muto Pure Chemicals Co, Japan) for 3 minutes. After sections were rinsed in phosphate-buffered saline, they were incubated with ImmunoBlock (Dainippon Sumitomo Pharma, Osaka, Japan) 1 hour in room air and incubated overnight at 4°C with 5% normal rabbit serum and rabbit polyclonal antibody to tenomodulin,[17,21] rabbit polyclonal antibody to VEGF-A (1:200 dilution; Santa Cruz Biotechnology, Santa Cruz, Calif), von Willebrand factor (vWF) (1:200 dilution; Laboratory Vision Corporation), elastin (1:50 dilution; Elastin Products Co), collagen type I (1:50 dilution; Rockland), matrix metalloproteinase (MMP)-1 (Daiichi Fine Chemical),[24] MMP-2 (Daiichi Fine Chemical),[24] MMP-3 (Daiichi Fine Chemical),[24] MMP-9 (Daiichi Fine Chemical),[24] MMP-13 (1:100 dilution; Biogenesis),[24] CD11b (1:200 dilution; BD PharMingen), CD14 (1:50 dilution; Santa Cruz Biotechnology), and vimentin (1:20 dilution; Sigma-Aldrich, St Louis, Mo). Immunohistochemical signals were detected by applying 0.05% 3,3′-diaminobenzidine tetrahydrochloride (Sigma-Aldrich) containing 0.01% hydrogen peroxide in 0.05 mol/L Tris-buffered saline (pH 7.6) as a chromogenic substrate. The sections were then counterstained with hematoxylin, dehydrated in a graded ethanol series, and mounted in Permount (Fisher Scientific).

For immunofluorescence studies, the sections were incubated with secondary antibodies conjugated with Alexa 488 or Alexa 546 (Molecular Probes, Carlsbad, Calif). Slides were observed under a confocal laser-scanning microscope (LSM 510 META; Carl Zeiss, Chester, Va). Optical sections were obtained at 1024×1024 pixel resolution and analyzed with the use of LSM software (Carl Zeiss). We substituted nonimmune rabbit serum for primary antibodies as a negative control for each immunostaining experiment.

Quantitative analysis of the stained area was performed by converting images to monochrome with optimum saturation and counting the black pixels with the use of NIH Image software.

Isolation of Adult Rabbit CTC Interstitial Cells

The hearts were dissected from anesthetized 12-week-old Japanese White rabbits. Primary culture of the CTC was examined by modifying the protocol for cardiac valvular interstitial cells[25] and Achilles tendons.[26] Briefly, the CTC was rapidly removed, and the superficial endothelial cells were removed by cotton swab, chopped under a stereomicroscope, and used for the explant culture. Pieces that measured 1×1 mm were cut from the tissue, placed in 12-well collagen-coated dishes (Iwaki), and grown in Dulbecco's modified Eagle's medium (Sigma-Aldrich) with 50% fetal bovine serum for 24 hours at 37°C. An additional 1 mL Dulbecco's modified Eagle's medium with 50% fetal bovine serum was added and left for another 24 hours at 37°C. After the medium and tissue pieces were removed, Dulbecco's modified Eagle's medium with 10% fetal bovine serum was added, and the cells were cultivated at 37°C. Medium was changed every 3 days. Conditioned medium was obtained from confluent CTC interstitial cells 3 days after the medium was changed and used in further analyses.

Cell Culture

Human coronary artery endothelial cells (HCAECs) were purchased from Takara Biotechnology, maintained according to the manufacturer's instructions, and used at passages 3 to 5 in the present study.

Human Samples

Samples comprising 16 CTC were collected from 15 patients undergoing mitral valve replacement or plasty due to its rupture and

1 autopsy patient (8 male and 8 female; mean age, 62.4±12.6 years). Samples were fixed immediately after removal in formaldehyde and then embedded in paraffin. For controls, 20 microscopically and macroscopically normal, noncalcified, smooth, and pliable mitral CTC were collected from 12 autopsied patients (10 male and 2 female; mean age, 62.7±16.5 years). The use of autopsied and surgical specimens of human tissue was approved by the institutional review board of Keio University and the National Cardiovascular Research Center.

Filing the Midlayer of CTC in a Canine Model

After administration of light anesthesia with intravenous injection of pentobarbital (30 mg/kg), adult beagle dogs weighing 14 to 16 kg (mean, 15.2±0.6 kg) were intubated, mechanically ventilated with room air by a Harvard respirator, and anesthetized with 3% sevoflurane and nitrous oxide. The right thoracotomy was performed at the fourth intercostal space, followed by generation of a pericardial cradle, and an extracorporeal bypass was created between the superior and inferior vena cava and the ascending aorta with an inline oxygenator. Both hemodynamics and gas exchange were monitored. The right atrium was opened, and the septal cusp of the tricuspid valve was directly shown. The surface of the several CTC of the septal cusp of tricuspid valve was filed out to remove the elastin layer. Then the heart was closed, extracorporeal bypass was removed, and the chest was closed. After 1 or 3 months, the dogs were anesthetized with pentobarbital and euthanized with KCl. The filed CTC were obtained (n=5, each group), and then the histological and immunohistochemical examinations were performed.

Other methods are described in the online-only Data Supplement.

Statistical Analysis

Values are presented as mean±SEM. Statistical significance was evaluated with the unpaired Student *t* test for comparisons between 2 mean values. Multiple comparisons between >3 groups were performed with an ANOVA test. A value of $P<0.05$ was considered significant.

The authors had fully access to and take full responsibility for the integrity of the data. All authors had read and agree to the manuscript as written.

Results

Expression of Tenomodulin in Normal CTC

Initially, we investigated whether tenomodulin was expressed in normal cardiac valves and CTC. Tenomodulin transcripts were first detected in the murine heart at embryonic day 14.5 and were expressed continuously in adulthood (Figure 1A). It was expressed specifically in the CTC but not in the atrium, ventricle, or cardiac valves (Figure 1B). Western blotting with antibodies specific for the C-terminal portion of tenomodulin identified the 45-kDa glycosylated and 40-kDa nonglycosylated forms of tenomodulin in porcine CTC; these proteins were also detected in the eye (Figure 1C). Interestingly, the CTC, but not the eye, was immunopositive for the 16-kDa C-terminal cleaved domain of tenomodulin, suggesting truncation of the C-terminus to produce the secreted form. Western blot analysis for the N-terminal domain of tenomodulin in the CTC revealed strong 29- and 24-kDa bands, as well as faint 45- and 40-kDa bands, whereas the eye contained mainly the 45- and 40-kDa fragments. Taken together, these results indicate that truncation of the C-terminal domain of tenomodulin occurs in a tissue-specific manner and that the truncated N-terminal domain persists in the CTC.

Immunohistochemistry of the murine heart localized tenomodulin to the CTC (Figure I in the online-only Data Supplement). Hematoxylin-eosin (HE) staining (Figure 2A), elastica van Gieson staining (Figure 2B), and immunohistochemistry revealed 3 layers in the normal human CTC, ie, the superficial endothelial layer (Figure 2E), the elastin-rich mid layer (Figure 2G), and the collagen type I–rich core layer (Figure 2H). This structure was consistent with that reported previously.[1] Tenomodulin was restricted to the elastin-rich mid layer (Figure 2C) and was not detected in the other layers. The normal CTC showed no expression of chondromodulin-I (Figure 2D) or VEGF-A (Figure 2F), and there was no abnormal vessel formation. Tenomodulin was deposited at the interstitial space of the elastin-rich layer, although it did not colocalize directly with elastin (Figure 2I).

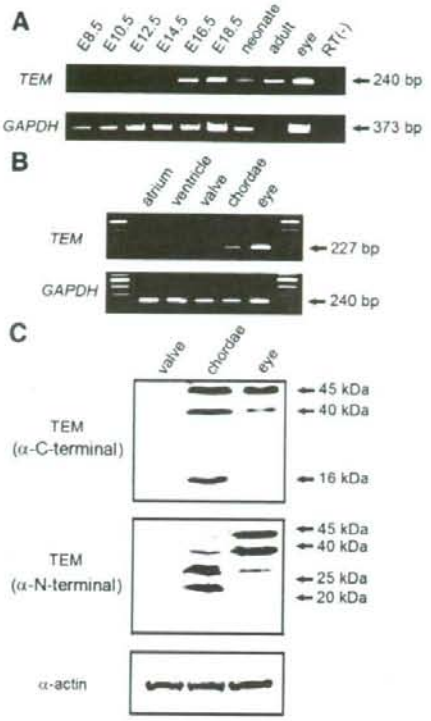

Figure 1. Expression of tenomodulin in CTC. A, Temporal expression of tenomodulin (TEM) in the mouse heart. RT-PCR was performed on samples from embryonic and adult hearts. Positive signals were seen in the embryonic heart from embryonic day (E) 14.5 onward. Adult mouse eyes were used as positive controls. B, RT-PCR of tenomodulin in the porcine heart. Tenomodulin mRNA was specifically expressed in the CTC but not in the atrium, ventricle, or cardiac valves. C, Western blot analysis for tenomodulin in the porcine cardiac valve and CTC with the use of antibody specific for the C-terminus (top panel) and N-terminus (middle panel) of tenomodulin. Eye was used as positive control. Note that the CTC expressed not only 45- and 40-kDa bands but also a 16-kDa band, although the eye expressed only the 45- and 40-kDa bands. This suggests that the C-terminal domain is processed in the CTC but not in the eye.

Tenomodulin Secreted From CTC Interstitial Cells Has Antiangiogenic Activity

We investigated whether CTC interstitial cells produce tenomodulin and the effect that this might have on the tube

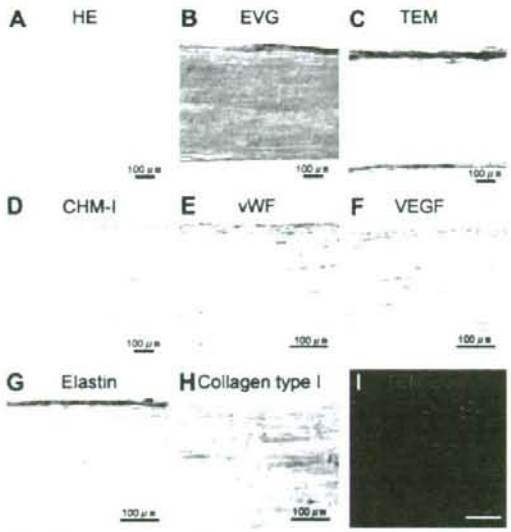

Figure 2. Localization of tenomodulin in normal human CTC. Normal human CTC was investigated by histological and immunohistochemical analyses. A, HE staining. B, Elastica van Gieson (EVG) staining. Immunohistochemistry for normal human CTC with anti-tenomodulin (TEM) (C), anti-chondromodulin-I (CHM-I) (D), anti-vWF (E), anti-VEGF-A (F), anti-elastin (G), and anti-collagen type I (H) antibodies. Tenomodulin was expressed at the elastin-rich mid layer of normal human CTC, and it did not colocalize directly with elastin (I).

morphogenesis of HCAECs. Primary CTC interstitial cells were obtained from explant cultures of rabbit CTC (Figure 3A). The explanted cells formed an orthogonal pattern of overgrowth. These cells were negative for the acetyl-LDL-DiI conjugate, which is consistent with CTC being composed of CTC interstitial cells. Immunostaining detected tenomodulin in the cytoplasm of CTC interstitial cells but not in NIH3T3 cells. RT-PCR confirmed that the cultured CTC interstitial cells expressed tenomodulin and that this expression could be inhibited by treatment with a specific small-interfering RNA (siRNA) (Figure 3B).

The HCAECs showed capillary-like tube formation on Matrigel (Figure 3C). These structures were less apparent after treatment with conditioned medium from CTC interstitial cell cultures (CIC-CM) compared with mock medium or the conditioned medium from NIH3T3 cell cultures (NIH3T3-CM). The HCAECs that were cultured in conditioned medium from siRNA-treated CTC interstitial cells regained the ability to form capillary-like structures. Conditioned media from cultures of NIH3T3 cells transfected with the C-terminal domain of tenomodulin (recombinant protein) similarly inhibited tube formation. Quantitative analysis revealed that CIC-CM inhibited tube formation by 58.3% and that tenomodulin-specific siRNA treatment recovered tube-forming capacity by 38.7% (Figure 3D).

Tenomodulin Secreted From CTC Interstitial Cells Inhibited the Migratory Capacity of the HCAECs

In a modified Boyden chamber, HCAECs cocultured with CTC interstitial cells lost their migratory capacity compared with that cocultured with NIH3T3 cells. Treatment of CTC interstitial cells with tenomodulin-specific siRNA allowed the HCAECs to regain partial migratory capacity (Figure 4A), whereas the control siRNA had no such effect. Coculturing with NIH3T3 cells transfected with the C-terminal domain of tenomodulin similarly inhibited migration. Quantitative analysis showed that CTC interstitial cells decreased the number of migrating cells by 73.2% and that specific siRNA recovered the migratory capacity by 36.6% (Figure 4B). These results imply a pivotal role for tenomodulin as an angiogenesis inhibitor in the CTC.

Marked Downregulation of Tenomodulin and Abnormal Vessel Formation in the Ruptured CTC

We examined specimens from 16 patients with CTC rupture (Figure 5A). The ruptured areas contained numerous large abnormal vessels in the mid layers and core layers, and there was marked tissue degeneration. Elastin was preserved, whereas tenomodulin was markedly downregulated in the ruptured area but not in remote nonruptured areas. These tenomodulin-poor areas expressed VEGF-A and contained the aforementioned large abnormal vessels. In addition, their inner surfaces were coated with vWF-positive endothelial cells rather than smooth muscle cells. Computer image analysis showed that the total cell numbers, vWF-positive cell numbers, and the percentages of VEGF-A–positive areas were markedly increased, whereas the proportions of tenomodulin-positive areas in the ruptured CTC were markedly decreased (Figure 5B to 5E). The adjacent nonruptured CTC obtained at autopsy and during mitral valve replacement revealed normal structures without abnormal vessel formation or aberrant MMP or VEGF-A expression (data not shown). These findings indicated that the CTC ruptures in a fragile area where numerous abnormal vessels are created and tenomodulin expression was locally downregulated.

Expression of MMPs and Cell Infiltration in the Ruptured CTC

The ruptured area of the CTC showed strong expression of MMP-1 and MMP-2 and moderate expression of MMP-13, which corresponded to the expression of VEGF-A (Figure 6A). In contrast, MMP-3 expression was weak, and MMP-9 was not detected. No MMP signals were detected in the normal CTC or in the nonruptured area. High numbers of inflammatory cells positive for CD11b, CD14, and vimentin infiltrated the ruptured area but not the normal CTC or the nonruptured area. The quantitative analyses are shown in Figure 6B to 6E. These findings suggest that abnormal vessel formation in the CTC is accompanied by MMP activation and infiltration of inflammatory cells.

Mechanical Stretching and Hypoxia Suppress the Expression of Tenomodulin by CTC Interstitial Cells

To investigate the cause of tenomodulin downregulation, we investigated whether tenomodulin expression by CTC interstitial cells was affected by various stimuli, such as mechanical stretching, hypoxia, or oxidative stress. CTC interstitial cells would be expected to experience these types of stimuli

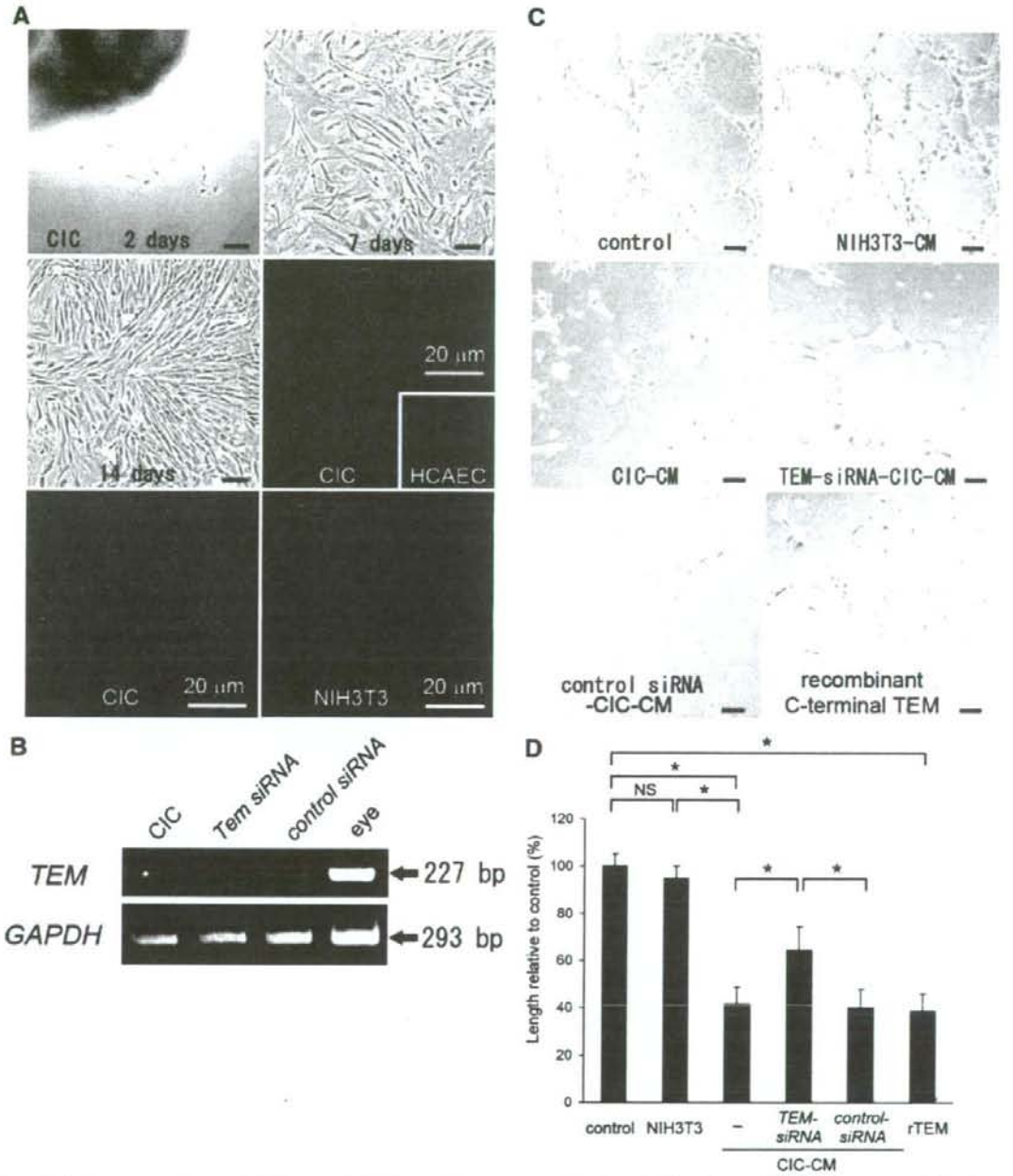

Figure 3. Expression of tenomodulin in CTC interstitial cells and its effect on tube formation in HCAECs. A, Rabbit CTC interstitial cells (CIC) after postexplant culture. At 7 days, CTC interstitial cells showed a cobblestone-like or spindle-like appearance. At 14 days, CTC interstitial cells exhibited a fibroblast-like appearance. Ex indicates explant of CTC. CTC interstitial cells were negative for acetyl-LDL-DiI staining; HCAECs are shown as a positive control (inset). Immunofluorescence staining of tenomodulin (TEM) in rabbit CTC interstitial cells and NIH3T3 cells is shown; nuclei were stained with ToPro-3. B, Effect of siRNA on tenomodulin expression in cultured CTC interstitial cells. RT-PCR for tenomodulin was performed. Lane 1, CIC; lane 2, CIC+siRNA specific to tenomodulin; lane 3, CIC+control siRNA; lane 4, eye for positive control of tenomodulin. C, Tube formation assay. CIC-CM inhibited tube formation of endothelial cells on Matrigel. Representative micrographs of tube formation of HCAECs are shown. Tube formation was significantly suppressed by CIC-CM but not by NIH3T3-CM (negative control). Treatment of CTC interstitial cells with siRNA specific to tenomodulin but not control siRNA reduced the CIC-CM–induced suppression. Recombinant C-terminal tenomodulin represented the conditioned medium of NIH3T3 cells transfected with C-terminal tenomodulin expression plasmids. D, Quantitative analysis of tube lengths in tube formation assay. *$P<0.01$ vs control.

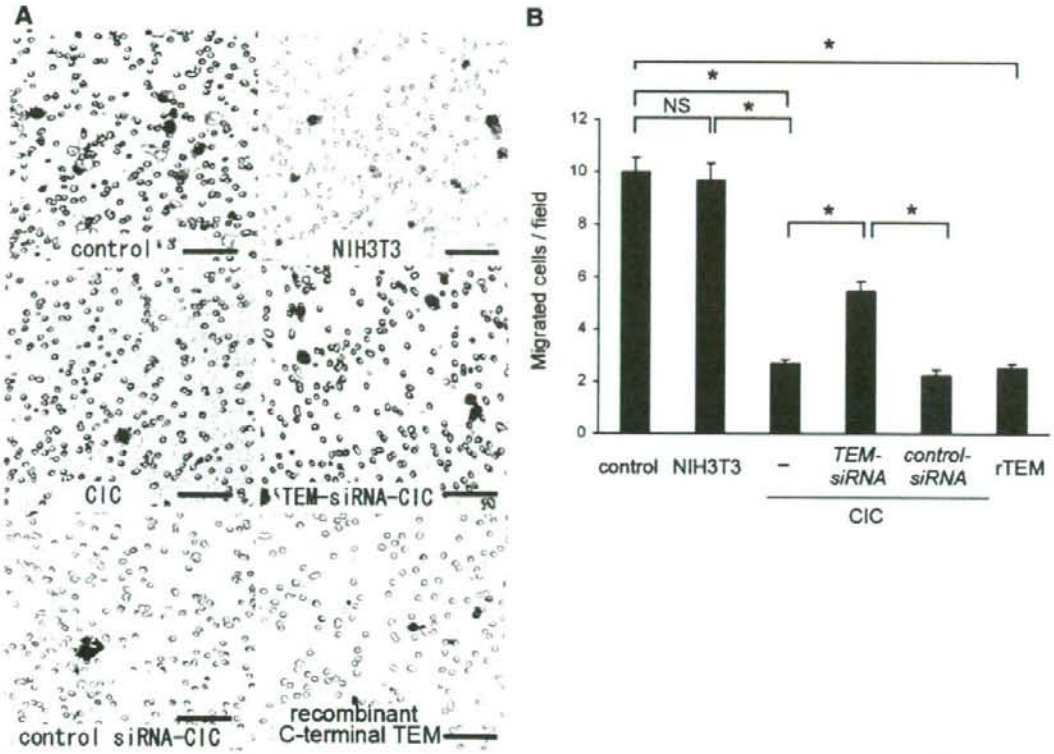

Figure 4. Effect of tenomodulin in CTC interstitial cells on HCAEC migration. A, Cell migration assay. CTC interstitial cells (CIC) abrogated HCAEC chemotaxis in vitro. HCAECs were inhibited from migrating when cocultured with CTC interstitial cells but not when cultured without cells (control) or with NIH3T3 cells (negative control). Treatment of CTC interstitial cells with siRNA specific to tenomodulin (TEM) but not control siRNA reduced the suppression of chemotaxis. Recombinant C-terminal tenomodulin represented the coculture with NIH3T3 cells transfected with C-terminal tenomodulin expression plasmids. B, The graph shows quantitative analysis of the migrated cell numbers in cell migration assay. *$P<0.01$ vs control.

when subjected to abnormal forces (as in hypertension) or during inflammation (as in infective endocarditis). Initially, we stimulated the CTC interstitial cells using a cell-stretching device, and 6 hours later, the expression of tenomodulin was not detectable (Figure IIA in the online-only Data Supplement). Next, CTC interstitial cells were incubated under the hypoxic condition of almost no oxygen. Although the cells were alive, the expression of tenomodulin was not detected as early as 1 hour later (Figure IIB in the online-only Data Supplement). Finally, CTC interstitial cells were treated with several concentrations of antimycin A, which mediates oxidative stress. Tenomodulin expression was observed at an antimycin A concentration <10 μg/mL but was undetectable at 30 μg/mL antimycin A (Figure IIC in the online-only Data Supplement). These findings suggest that various stimuli, such as mechanical stretching, hypoxia, and oxidative stress, cause the down regulation of tenomodulin expression in CTC.

Absence of the Tenomodulin Layer Induces Angiogenesis and MMP Activation

We investigated the effects of the tenomodulin layer on angiogenesis and MMP activation in the collagen-rich core layer. The CTC of the tricuspid valve was examined in an anesthetized canine model, and the tenomodulin-rich layer was removed by filing (Figure 7A). Hemodynamic measurement revealed that there were no significant differences in heart rate, systolic pressure, diastolic pressure, pulmonary arterial pressure, pulmonary capillary wedge pressure, right ventricular systolic pressure, right atrial pressure, and cardiac output between the control (presurgery) dogs and the dogs at 3 months after surgery. Color Doppler echocardiography revealed no significant increases in tricuspid regurgitation at 3 months after surgery.

HE staining and immunostaining for vWF revealed abnormal vessel formation in the core layer next to the surgically filed tenomodulin-deficient area at 3 months (Figure 7B, 7C). Immunohistochemical analyses were performed at 1 and 3 months, at which point the acute inflammation had terminated. VEGF-A, MMP-1, MMP-2, and MMP-13 were observed from 1 month, with their expression extending to ≈15% of the core layer depth (Figure 7D). At 3 months, the expression of these factors was stronger and extended to 37% of the core layer depth. Moreover, abnormal neovascularization was observed only at 3 months, indicating that angiogenesis and MMP activation are caused by loss of the tenomodulin-rich layer rather than operation-induced inflammation (Figure 7E to 7G).

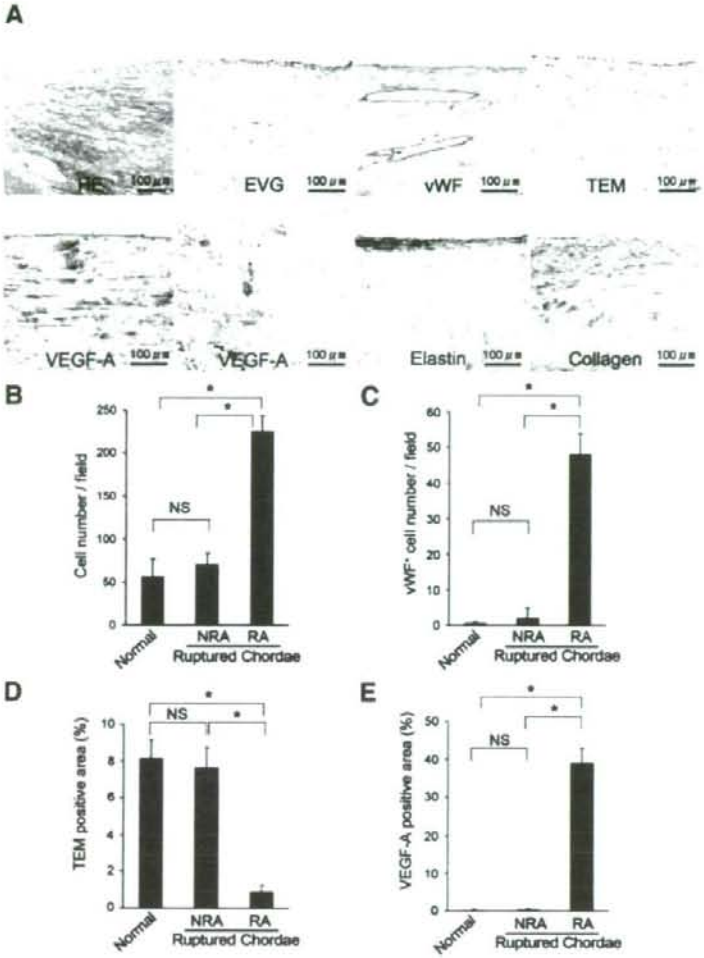

Figure 5. A, Representative histology and immunohistochemistry of the ruptured CTC. Abbreviations are as in Figure 2. The ruptured areas of CTC did not express tenomodulin, whereas they strongly expressed VEGF-A. Note that many abnormal large vessels were apparent in the ruptured area of CTC, and they were covered with vWF$^+$ endothelial cells. Elastica van Gieson (EVG) staining and immunostaining for elastin and collagen type I revealed that the laminar structure was maintained in the ruptured area of CTC, although they were destroyed. B, Quantitative analysis of the number of cells in the normal, nonruptured area (NRA) and ruptured areas (RA) of disrupted CTC. C, Quantitative analysis of the vWF$^+$ cell number. D, Quantitative analysis of the percentage of tenomodulin$^+$ area in normal, NRA, or RA of CTC. E, Quantitative analysis of the percentage of VEGF-A$^+$ area in normal, NRA, or RA of CTC. *$P<0.01$ vs control.

Discussion

Despite their clinical importance, little is known about the mechanisms underlying VHDs.[27-29] The present study reveals a key role for tenomodulin as a potent antiangiogenic factor in the prevention of atrioventricular valvular regurgitation after CTC rupture. We show for the first time that both the C-terminal and N-terminal domains of tenomodulin are expressed persistently in the mid layer of normal CTC, whereas these proteins are downregulated in the diseased CTC. Moreover, the cleaved C-terminal domain of tenomodulin secreted from CTC interstitial cells is a critical antagonist of angiogenesis. Because cardiac valves are flow-regulating tissues in a dynamic chambered pump, the CTC are subjected to mechanical stress[30] and damage to the endothelial cell lining of the outer layer. Tenomodulin probably protects the CTC from the inflammation and vascularization that result from mechanical damage. To confirm this hypothesis, we analyzed the tenomodulin expression profiles of the CTC in the normal and diseased states.

The observed expression patterns and biological activities suggest that tenomodulin protects against both angiogenesis and degeneration of the core layer, analogous to the surface coating applied to steel to prevent internal corrosion. Indeed, observations of the ruptured CTC revealed that VEGF-A and MMPs were strongly activated with increased formation of abnormal vessels, resulting in degeneration of the CTC. More importantly, these areas of degeneration corresponded to regions of local absence of tenomodulin. The dog experiments clearly support our hypothesis that angiogenesis and degeneration occur progressively in areas from which the tenomodulin layer has been removed. These findings suggest that CTC rupture is not accidental but can occur when and where the CTC is weakened by angiogenesis, MMP activation, and the infiltration of inflammatory cells secondary to the loss of or damage to the tenomodulin layer. The molecular mechanism through which a local deficit of tenomodulin causes VEGF-A expression remains unknown. We assume that

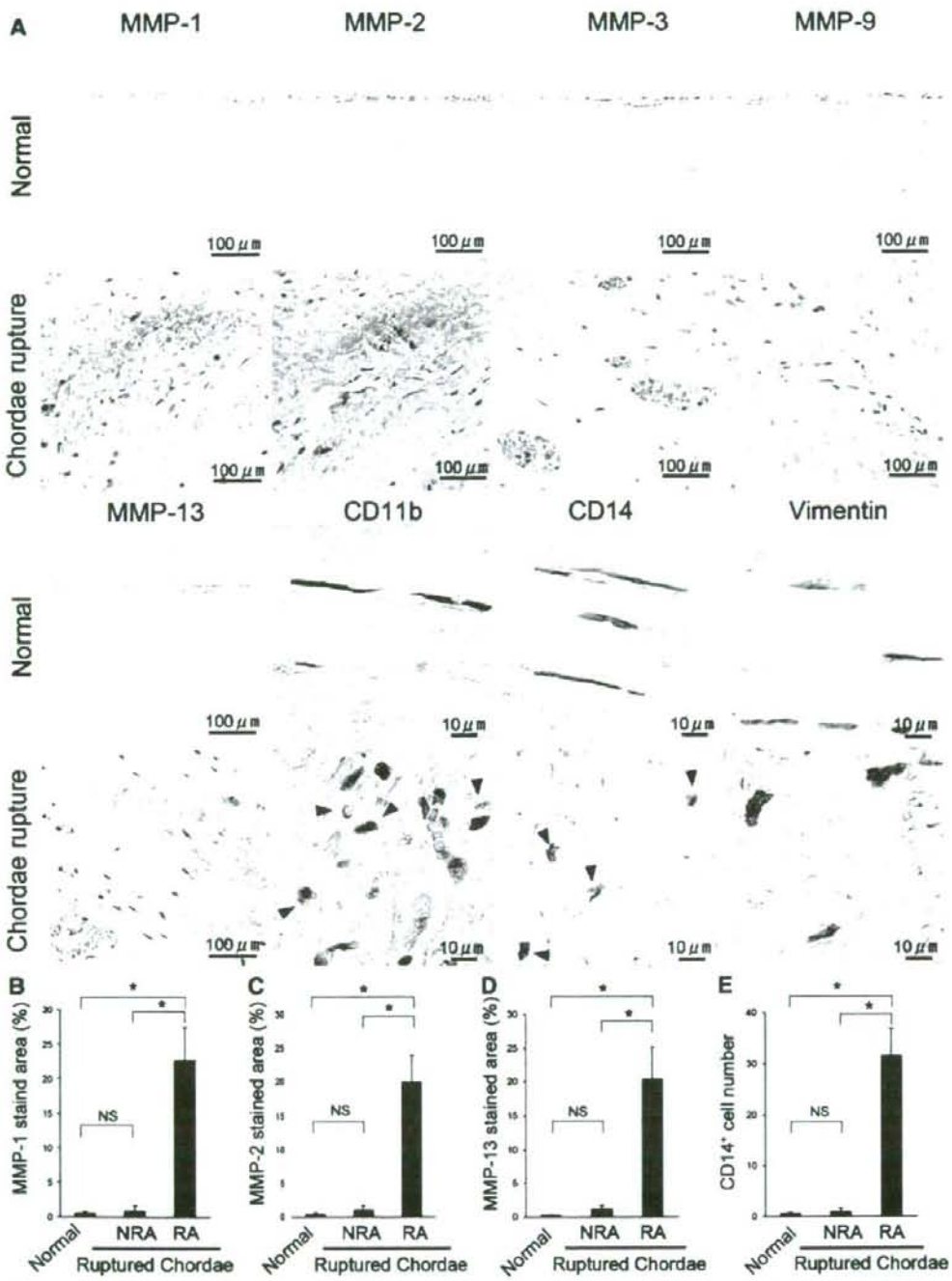

Figure 6. A, Immunohistochemistry of CTC from human autopsies and surgical samples with the use of anti-MMP-1, -MMP-2, -MMP-3, -MMP-9, -MMP-13, -CD11b, -CD14, and -vimentin antibodies. Normal represented the samples from autopsies with normal CTC. The chordae rupture represented the ruptured area of the CTC from surgical samples. B, Quantitative analysis of the percentage of MMP-1–immunostained area in the normal autopsied sample, the nonruptured area (NRA), and ruptured area (RA) of surgical CTC specimen. C, Quantitative analysis of the percentage of MMP-2–immunostained area. D, Quantitative analysis of the percentage of MMP-13–immunostained area. E, Quantitative analysis of the number of $CD14^+$ cells in CTC. *$P<0.01$ vs control.

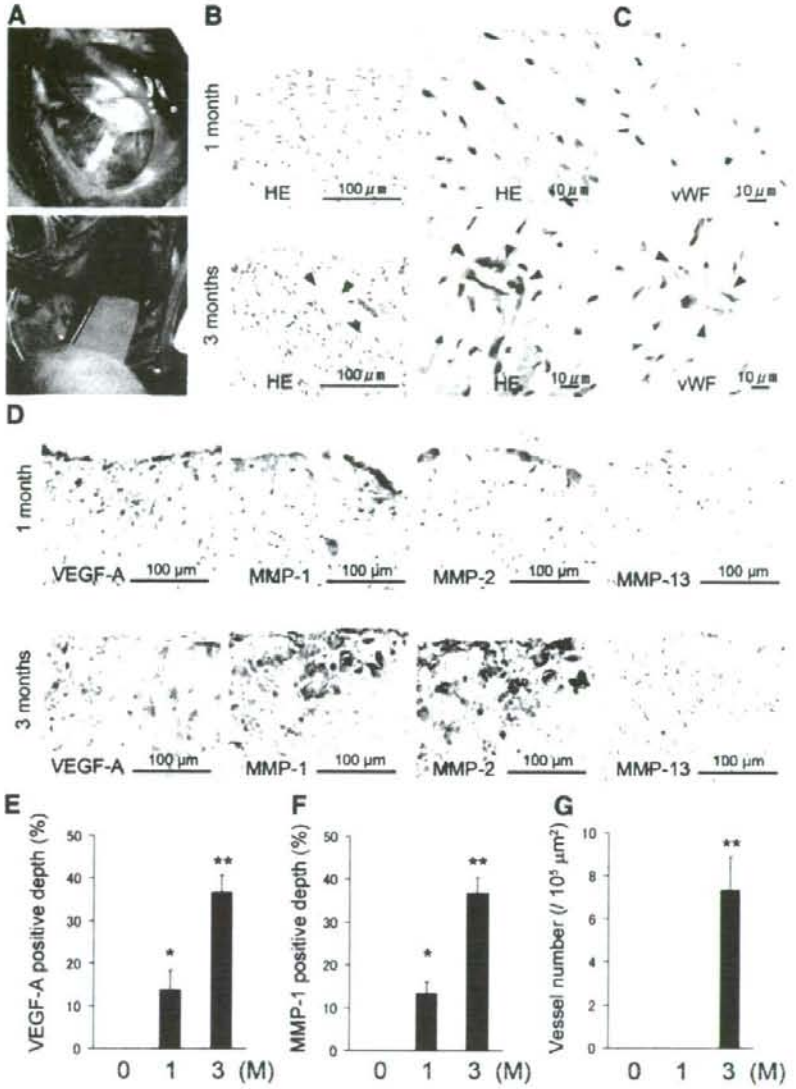

Figure 7. A, Operator's view of the CTC in the tricuspid valve (the septal cusp) in canine model (top panel). The superficial and mid layers of CTC were removed by filing (bottom panel). B, HE staining of the CTC at 1 and 3 months. Note that abnormal small vessel was observed at 3 months. C, Immunohistochemistry for vWF on CTC. Abnormal vessel at 3 months was covered with vWF$^+$ endothelial cells. D, Immunohistochemistry for VEGF-A, MMP-1, MMP-2, and MMP-13 is demonstrated. E, Quantitative analysis for VEGF-A–positive depth compared with the depth of core layer. M indicates month. F, Quantitative analysis for MMP-1–positive depth compared with the depth of core layer. G, Quantitative analysis of the abnormal vessel numbers. $^*P<0.01$, $^{**}P<0.01$ vs control (sham operation, 0 month).

either the downregulation of tenomodulin in CTC interstitial cells or the loss of tenomodulin-producing cells owing to long-standing mechanical stress or inflammation leads to the infiltration of endothelial cells and inflammatory cells, resulting in the activation of MMPs and the expression of VEGF-A. Tenomodulin plays a major role as an antiangiogenic factor in CTC; however, our present data do not exclude the possibility of the existence of other antiangiogenic factors. This should be clarified in the future. We propose that tenomodulin loss occurs after (1) acute inflammation, as in infective endocarditis and rheumatic fever, and (2) excessive mechanical stress to valves, as in trauma, hypertension,[31] and mitral valve prolapse.

The Achilles tendon is one of the most common sites of rupture. It ruptures spontaneously in the majority of patients, without substantial trauma.[32] Local vascularization is implicated in the etiology of this rupture[33,34]; high levels of VEGF-A are expressed by the tenocytes of

ruptured Achilles tendons but not by the tenocytes of normal adult Achilles tendons.[35,36] Hypercellularity, marked vessel formation, and increased MMP expression lead to weakening of the normal tendon structure and subsequent decrease in the mechanical strain tolerance, leading to spontaneous rupture.[36,37] The similarities between these earlier findings and those of the present study suggest that locally augmented mechanical stress or inflammation causes local defects in tenomodulin and induces VEGF-A expression, which may lead to MMP activation, angiogenesis, and degeneration of the CTC to the extent that it ruptures. The present findings support the notion of preclinical investigations of tenomodulin and proteins of similar function as therapeutic agents for the prevention of VHD due to rupture or elongation of the CTC. Understanding these mechanisms should form the basis for new therapeutic regimens for the treatment of VHD.

Sources of Funding

This study was supported in part by research grants from the Ministry of Education, Science, and Culture, Japan, and by the Program for Promotion of Fundamental Studies in Health Science of the National Institute of Biomedical Innovation, Japan.

Disclosures

None.

References

1. Millington-Sanders C, Meir A, Lawrence L, Stolinski C. Structure of chordae tenidineae in the left ventricle of the human heart. *J Anat*. 1998;192:573–581.
2. Soini Y, Salo T, Satta J. Angiogenesis is involved in the pathogenesis of nonrheumatic aortic valve stenosis. *Hum Pathol*. 2003;34:756–763.
3. Yamauchi R, Tanaka M, Kume N, Minami M, Kawamoto T, Togi K, Shimaoka T, Takahashi S, Yamaguchi J, Nishina T, Kitaichi M, Komeda M, Manabe T, Yonehara S, Kita T. Upregulation of SR-PSOX/CXCL16 and recruitment of CD8+ T cells in cardiac valves during inflammatory valvular heart disease. *Arterioscler Thromb Vasc Biol*. 2004;24:282–287.
4. Mohler ER III, Gannon F, Reynolds C, Zimmerman R, Keane MG, Kaplan FS. Bone formation and inflammation in cardiac valves. *Circulation*. 2001;103:1522–1528.
5. Hiraki Y, Inoue H, Iyama K, Kamizono A, Ochiai M, Shukunami C, Iijima S, Suzuki F, Kondo J. Identification of chondromodulin I as a novel endothelial cell growth inhibitor: purification and its localization in the avascular zone of epiphyseal cartilage. *J Biol Chem*. 1997;272:32419–32426.
6. Hiraki Y, Kono T, Sato M, Shukunami C, Kondo J. Inhibition of DNA synthesis and tube morphogenesis of cultured vascular endothelial cells by chondromodulin-I. *FEBS Lett*. 1997;415:321–324.
7. Nakamichi Y, Shukunami C, Yamada T, Aihara K, Kawano H, Sato T, Nishizaki Y, Yamamoto Y, Shindo M, Yoshimura K, Nakamura T, Takahashi N, Kawaguchi H, Hiraki Y, Kato S. Chondromodulin I is a bone remodeling factor. *Mol Cell Biol*. 2003;23:636–644.
8. Yamana K, Wada H, Takahashi Y, Sato H, Kasahara Y, Kiyoki M. Molecular cloning and characterization of CHM1L, a novel membrane molecule similar to chondromodulin-I. *Biochem Biophys Res Commun*. 2001;280:1101–1106.
9. Yoshioka M, Yuasa S, Matsumura K, Kimura K, Shiomi T, Kimura N, Shukunami C, Okada Y, Mukai M, Shin H, Yozu R, Sata M, Ogawa S, Hiraki Y, Fukuda K. Chondromodulin-I maintains cardiac valvular function by preventing angiogenesis. *Nat Med*. 2006;12:1151–1159.
10. Chimal-Monroy J, Rodriguez-Leon J, Montero JA, Ganan Y, Macias D, Merino R, Hurle JM. Analysis of the molecular cascade responsible for mesodermal limb chondrogenesis: Sox genes and BMP signaling. *Dev Biol*. 2003;257:292–301.
11. Lincoln J, Alfieri CM, Yutzey KE. Development of heart valve leaflets and supporting apparatus in chicken and mouse embryos. *Dev Dyn*. 2004;230:239–250.
12. Chiquet M, Fambrough DM. Chick myotendinous antigen: a monoclonal antibody as a marker for tendon and muscle morphogenesis. *J Cell Biol*. 1984;98:1926–1936.
13. Schweitzer R, Chyung JH, Murtaugh LC, Brent AE, Rosen V, Olson EN, Lassar A, Tabin CJ. Analysis of the tendon cell fate using Scleraxis, a specific marker for tendons and ligaments. *Development*. 2001;128:3855–3866.
14. Lincoln J, Alfieri CM, Yutzey KE. BMP and FGF regulatory pathways control cell lineage diversification of heart valve precursor cells. *Dev Biol*. 2006;292:292–302.
15. Zhao B, Etter L, Hinton RB Jr, Benson DW. BMP and FGF regulatory pathways in semilunar valve precursor cells. *Dev Dyn*. 2007;236:971–980.
16. Shukunami C, Oshima Y, Hiraki Y. Molecular cloning of tenomodulin, a novel chondromodulin-I related gene. *Biochem Biophys Res Commun*. 2001;280:1323–1327.
17. Oshima Y, Shukunami C, Honda J, Nishida K, Tashiro F, Miyazaki J, Hiraki Y, Tano Y. Expression and localization of tenomodulin, a transmembrane type chondromodulin-I-related angiogenesis inhibitor, in mouse eyes. *Invest Ophthalmol Vis Sci*. 2003;44:1814–1823.
18. Shukunami C, Oshima Y, Hiraki Y. Chondromodulin-I and tenomodulin: a new class of tissue-specific angiogenesis inhibitors found in hypovascular connective tissues. *Biochem Biophys Res Commun*. 2005;333:299–307.
19. Shukunami C, Takimoto A, Oro M, Hiraki Y. Scleraxis positively regulates the expression of tenomodulin, a differentiation marker of tenocytes. *Dev Biol*. 2006;298:234–247.
20. Hiraki Y, Shukunami C. Angiogenesis inhibitors localized in hypovascular mesenchymal tissues: chondromodulin-I and tenomodulin. *Connect Tissue Res*. 2005;46:3–11.
21. Docheva D, Hunziker EB, Fassler R, Brandau O. Tenomodulin is necessary for tenocyte proliferation and tendon maturation. *Mol Cell Biol*. 2005;25:699–705.
22. Oshima Y, Sato K, Tashiro F, Miyazaki J, Nishida K, Hiraki Y, Tano Y, Shukunami C. Anti-angiogenic action of the C-terminal domain of tenomodulin that shares homology with chondromodulin-I. *J Cell Sci*. 2004;117:2731–2744.
23. Funaki H, Sawaguchi S, Yaoeda K, Koyama Y, Yaoita E, Funaki S, Shirakashi M, Oshima Y, Shukunami C, Hiraki Y, Abe H, Yamamoto T. Expression and localization of angiogenic inhibitory factor, chondromodulin-I, in adult rat eye. *Invest Ophthalmol Vis Sci*. 2001;42:1193–1200.
24. Fujimoto N, Iwata K. Use of EIA to measure MMPs and TIMPs. *Methods Mol Biol*. 2001;151:347–358.
25. Zacks S, Rosenthal A, Granton B, Havenith M, Opas M, Gotlieb AI. Characterization of Cobblestone mitral valve interstitial cells. *Arch Pathol Lab Med*. 1991;115:774–779.
26. Pufe T, Petersen W, Kurz B, Tsokos M, Tillmann B, Mentlein R. Mechanical factors influence the expression of endostatin—an inhibitor of angiogenesis—in tendons. *J Orthop Res*. 2003;21:610–616.
27. Chalajour F, Treede H, Ebrahimnejad A, Lauke H, Reichenspurner H, Ergun S. Angiogenic activation of valvular endothelial cells in aortic valve stenosis. *Exp Cell Res*. 2004;298:455–464.
28. Freed LA, Acierno JS Jr, Dai D, Leyne M, Marshall JE, Nesta F, Levine RA, Slaugenhaupt SA. A locus for autosomal dominant mitral valve prolapse on chromosome 11p15.4. *Am J Hum Genet*. 2003;72:1551–1559.
29. Sedransk KL, Grande-Allen KJ, Vesely I. Failure mechanics of mitral valve chordae tendineae. *J Heart Valve Dis*. 2002;11:644–650.
30. Rodriguez F, Langer F, Harrington KB, Tibayan FA, Zasio MK, Cheng A, Liang D, Daughters GT, Covell JW, Criscione JC, Ingels NB, Miller DC. Importance of mitral valve second-order chordae for left ventricular geometry, wall thickening mechanics, and global systolic function. *Circulation*. 2004;110:II115–II122.
31. Lin TH, Su HM, Voon WC, Lai HM, Yen HW, Lai WT, Sheu SH. Association between hypertension and primary mitral chordae tendinae rupture. *Am J Hypertens*. 2006;19:75–79.
32. Jozsa LG, Kannus P. *Human Tendons: Anatomy, Physiology, and Pathology*. Champaign, Ill: Human Kinetics; 1997.
33. Movin T, Gad A, Reinholt FP, Rolf C. Tendon pathology in long-standing achillodynia: biopsy findings in 40 patients. *Acta Orthop Scand*. 1997;68:170–175.